

The effect of varying levels of surfactant on the reactive uptake of N_2O_5 to aqueous aerosol

V. F. McNeill¹, J. Patterson², G. M. Wolfe², and J. A. Thornton¹

¹Department of Atmospheric Sciences, University of Washington, Seattle, Washington, 98195, USA

²Department of Chemistry, University of Washington, Seattle, Washington, 98195, USA

Received: 10 November 2005 – Published in Atmos. Chem. Phys. Discuss.: 2 January 2006

Revised: 20 March 2006 – Accepted: 20 March 2006 – Published: 22 May 2006

Abstract. Recent observations have detected surface active organics in atmospheric aerosols. We have studied the reaction of N_2O_5 on aqueous natural seawater and NaCl aerosols as a function of sodium dodecyl sulfate (SDS) concentration to test the effect of varying levels of surfactant on gas-aerosol reaction rates. SDS was chosen as a proxy for naturally occurring long chain monocarboxylic acid molecules, such as palmitic or stearic acid, because of its solubility in water and well-characterized surface properties. Experiments were performed using a newly constructed aerosol flow tube coupled to a chemical ionization mass spectrometer for monitoring the gas phase, and a differential mobility analyzer/condensation particle counter for determining aerosol surface area. We find that the presence of ~ 3.5 wt% SDS in the aerosol, which corresponds to a monolayer surface coverage of $\sim 2 \times 10^{14}$ molecules cm^{-2} , suppresses the N_2O_5 reaction probability, $\gamma^{\text{N}_2\text{O}_5}$, by approximately a factor of ten, independent of relative humidity. Consistent with this observation is a similar reduction in the rate of ClNO_2 product generation measured simultaneously. However, the product yield remains nearly constant under all conditions. The degree of suppression is strongly dependent on SDS content in the aerosol, with no discernable effect at 0.1 wt% SDS, but significant suppression at what we predict to be submonolayer coverages with 0.3–0.6 wt% SDS on NaCl and natural seawater aerosols, respectively.

1 Introduction

Organic material is a major component of natural and anthropogenic atmospheric aerosols (McMurry, 2000). In the past few decades, hundreds of organic species found in atmospheric particles have been identified, although the major-

ity of organic aerosol mass often remains unspiciated (Saxena and Hildemann, 1996; McMurry, 2000; Jacobson et al., 2000). There has been a renewed interest in the sources and fates of surface active organic molecules due to their potential impact on gas-aerosol interfacial chemistry. Surface active films were first extracted from sea salt aerosol by Blanchard (1964) over 40 years ago. Recent studies have shown the presence of fatty acids in marine aerosol sampled over the North Atlantic (O'Dowd et al., 2004; Cavalli et al., 2004) and northern North Pacific (Mochida et al., 2002), with maximum concentrations occurring during periods of high biological productivity. Soft X-ray spectromicroscopy (Russell et al., 2002) and TOF-SIMS (Tervahattu et al., 2002; Peterson and Tyler, 2003) have revealed organic coatings on dried sea salt particles. Tervahattu et al. (2002) used TOF-SIMS to identify the main component of the organic layer as palmitic acid. It has been postulated that marine aerosol may obtain a surfactant component from an organic-rich surface layer that is present on seawater during periods of high biological activity via a bubble-bursting mechanism (Gershey, 1983; Mochida et al., 2002). On aqueous atmospheric aerosol, these surfactant molecules are thought to form an organic surface layer in an “inverted micelle” configuration, possibly affecting the transport of molecules across the air-aerosol interface and surface reactions (Gill et al., 1983; Ellison et al., 1999).

While it is well-known that the presence of a long-chain fatty acid layer inhibits the evaporation of a macroscopic water film (Rideal, 1925; Archer and La Mer, 1955; Rosano and La Mer, 1956), the effect of surface active organics on the interaction of aerosols with gas phase species, particularly in reactive systems, remains poorly characterized. In a recent molecular beam scattering (TOF-MS) study, Lawrence et al. (2005b) found that a butanol coating on supercooled deuterated sulfuric acid films ($T=213$ K) did not inhibit proton exchange by HCl and HBr, and in fact suggest that the hydrophilic head groups of the butanol may provide additional

Correspondence to: J. A. Thornton
(thornton@atmos.washington.edu)

sites for interaction with the adsorbate. Short-chained surfactants such as butanol are known to form less tightly packed films and provide a lower barrier to water evaporation than longer-chained surfactants (Archer and La Mer, 1955; Rosano and La Mer, 1956). Monolayer levels of fatty acids at the air-water interface were found by Mmereki et al. (2004) to inhibit the Langmuir-Hinshelwood surface reaction between ozone and adsorbed anthracene, a polycyclic aromatic hydrocarbon, while a monolayer of 1-octanol was observed to enhance the reaction rate (Mmereki and Donaldson, 2003). Most recently, Thornton and Abbatt (2005) found that the presence of hexanoic acid decreased the N_2O_5 reactive uptake coefficient on artificial seawater (ASW) aerosol by a factor of 3–4 at 70% relative humidity (*RH*). To our knowledge, these are the only studies of the effect of monolayer organic films on gas-aerosol reactive uptake kinetics, though it has been shown that a multilayer hydrophobic shell (≥ 15 nm) on aqueous inorganic aerosol causes a significant reduction in the reactive uptake of N_2O_5 (Folkers et al., 2003).

In a continuing effort to elucidate the impact of aerosol organic matter on important heterogeneous reactions, we examined the reaction of N_2O_5 on aqueous natural seawater and NaCl aerosol containing trace amounts (≤ 10 wt%) of sodium dodecyl sulfate, SDS ($\text{C}_{12}\text{H}_{25}\text{OSO}_3\text{Na}$). Our goal was to determine the effect of sub-monolayer surfactant coatings on the kinetics and product yields of this reaction. Our choice of aqueous natural seawater and NaCl aerosol was motivated in part by the fact that the reaction of N_2O_5 with aqueous sea salt aerosols is a sink for nitrogen oxides and a potential source of the chlorine radical in the polluted marine boundary layer. Although discrepancies remain with regard to the product yields of this reaction on aerosols (Behnke et al., 1997; Schweitzer et al., 1998; Thornton and Abbatt, 2005), the reaction is relatively well-characterized (Behnke et al., 1997; Schweitzer et al., 1998; Hoffmann et al., 2003; Stewart et al., 2004; Thornton and Abbatt, 2005) and provides a useful starting point to assess the role of surfactants. The ClNO_2 product, which volatilizes readily from sub-micron aerosol, provides an additional indicator of the reaction pathways occurring in the aerosol.

Given the lack of direct kinetic studies of gas-aerosol interactions where surfactants are present, SDS was chosen as a proxy for natural organic surfactant molecules because it is readily soluble in water and because the SDS-NaCl- H_2O system has been characterized in bulk solutions (Matijevic and Pethica, 1958; Rehfeld, 1967; Persson et al., 2003; Sorjamaa et al., 2004; Li et al., 1998). SDS is similar to fatty acids in that it contains a long aliphatic tail on a polar head group whose anionic character is likely pH dependent. The aliphatic tail of SDS is analogous to that of lauric acid (C_{12}), which has been identified in both natural marine (Mayol-Bracero et al., 2001) and continental aerosols (Gill et al., 1983; Duce et al., 1983; Rogge et al., 1993). We find that the N_2O_5 reaction probability decreases with increasing SDS mass fraction, and eventually plateaus at 3.5 wt% SDS, be-

yond which no further decrease is observed. These results suggest that even small quantities of a C_{12} surfactant on the surface of aqueous atmospheric aerosol have the potential to inhibit the rates of gas-aerosol mass transfer and heterogeneous chemistry.

2 Experimental

Experiments were performed using a recently constructed aerosol flow tube coupled to a custom-built chemical ionization mass spectrometer (CIMS) for monitoring the gas phase, and a differential mobility analyzer/condensation particle counter (Grimm Technologies) for determining aerosol surface area. The experimental setup and procedure closely resembles that described in detail previously (Thornton et al., 2003; Thornton and Abbatt, 2005), but we highlight significant differences below.

2.1 Aerosol generation and characterization

Sub-micron aqueous NaCl aerosol were generated by atomizing a 0.05 M solution of NaCl in deionized water using a commercial constant output atomizer (TSI). We chose to use NaCl in addition to natural seawater due to lower wall losses of N_2O_5 which allow us to better quantify slow aerosol reactions. The presence of Mg^{2+} in seawater aerosol appears to lead to a greater retention of water on the reactor walls upon aerosol impaction (Cziczo and Abbatt, 2000). To generate SDS-doped NaCl aerosol, small quantities of a stock solution prepared from SDS crystals and deionized water were added to the 0.05 M NaCl solution to create mixtures with 10^{-5} M– 10^{-3} M SDS which were then atomized. Similarly, sub-micron natural seawater (NSW) aerosol were generated by atomizing a dilute solution of natural seawater in deionized water (1:7.3). This dilution was chosen to create a 0.05 M solution assuming a NaCl concentration of 0.415 M in natural seawater. The sample was taken from the Caribbean Sea ($18^\circ 30.09' \text{N}$, $64^\circ 21.47' \text{W}$) in July 2005. SDS-doped NSW aerosol was generated using the same procedure as the SDS-doped NaCl aerosol.

The atomizer output (~ 1 slpm) was mixed with a ~ 4 slpm humidified N_2 flow and transported (~ 10 s) to the kinetics flow tube. The *RH* of the equilibrated N_2 /aerosol stream was monitored at the inlet to the aerosol flow tube with a commercial hygrometer (Fisher Scientific, Vaisala). Reported values for *RH* are accurate to within 2%. The humidified aerosol stream amounted to $>94\%$ of the total flow in the flow tube, and thus the *RH* inside the reactor is assumed to be that of the aerosol flow. Experiments were performed at 50%–72% *RH*. We did not perform experiments at *RH* < 50% because NaCl aerosol crystallize at 43% *RH* (Cziczo and Abbatt, 2000) and our goal was to assess the effect of SDS on aqueous particles.

Because water evaporates from aerosol when the 100% *RH* atomizer output combines with the drier bulk flow, the

aerosol become greatly concentrated relative to the bulk atomizer solution. Following Tang et al. (1997), at 62% *RH*, an aqueous NaCl aerosol will be 8.8 M NaCl. Assuming the same proportional increase in concentration (176 \times), we estimate that 0.001 M SDS in the atomizer solution corresponds to 0.176 M SDS in the aerosol. Based on a volume of 1.1×10^{-17} L calculated using the surface area weighted average particle radius, 0.176 M SDS corresponds to an average of 1.2×10^6 SDS molecules/particle. To avoid confusion concerning bulk-surface partitioning of SDS and the total amount of SDS available per particle, we will refer to SDS concentration as a solute mass fraction (wt%), instead of molarity. Thus, atomizing a solution containing 0.001 M SDS yields aerosol at 62% *RH* that are 10 wt% SDS.

The aerosol population was continuously sampled at the exit of the kinetics flow tube by a differential mobility analyzer (DMA) coupled to an ultra-fine condensation particle counter (CPC). So that the *RH* of the DMA sheath flow was similar to the sample flow, the DMA/CPC drew humidified bulk flow for ~ 1 h prior to starting experiments. The aerosol, with and without SDS present, exhibited a log-normal size distribution with a typical geometric standard deviation of 2.0. NaCl aerosol had an average mean surface area-weighted particle radius, r_p , of 140 ± 10 nm, while for NSW aerosol, $r_p = 160 \pm 10$ nm. Representative number and surface area-weighted aerosol size distributions for aqueous NaCl aerosol at 61% *RH* with and without 10 wt% SDS are shown in Fig. 1. Total surface area was typically between 9×10^{-4} – 2.2×10^{-3} cm² cm⁻³ for NaCl and NSW aerosol and between 5×10^{-4} cm² cm⁻³– 1.5×10^{-3} cm² cm⁻³ with SDS present. The lower surface area concentrations were used with the SDS mixtures to minimize foaming in the atomizer outlet. In addition, at the highest surface area concentrations generated with the SDS mixtures, there was a noticeable shift in the r_p to higher sizes (300–400 nm). As the DMA is unable to accurately size aerosol above ~ 800 nm, the measured surface area under these conditions may be an underestimate causing our reported reaction probabilities to be biased high by at most 50%. This issue does not impact our conclusions.

2.2 N₂O₅ synthesis and delivery

N₂O₅ was synthesized using NO₂ and O₃, and was collected at -83°C . O₃ was generated using a pen-ray lamp (UVP). The N₂O₅ sample was stored at $\sim -50^\circ\text{C}$ using a cold finger (NESLAB). During experiments, the sample was kept between -70°C and -74°C . The vapor pressure of N₂O₅ at -70°C is estimated to be 0.006 ± 0.003 Torr (Thornton et al., 2003). N₂O₅ was delivered to the flow tube by flowing 5 sccm dry N₂ through the trap. The saturated flow was then combined with a 100 sccm N₂ carrier flow and transported through ~ 3 m of 3 mm OD PFA tubing into the flow tube reactor. Typical initial concentrations in the flow reactor were 5.5×10^{11} molecules cm⁻³ (22 ppb).

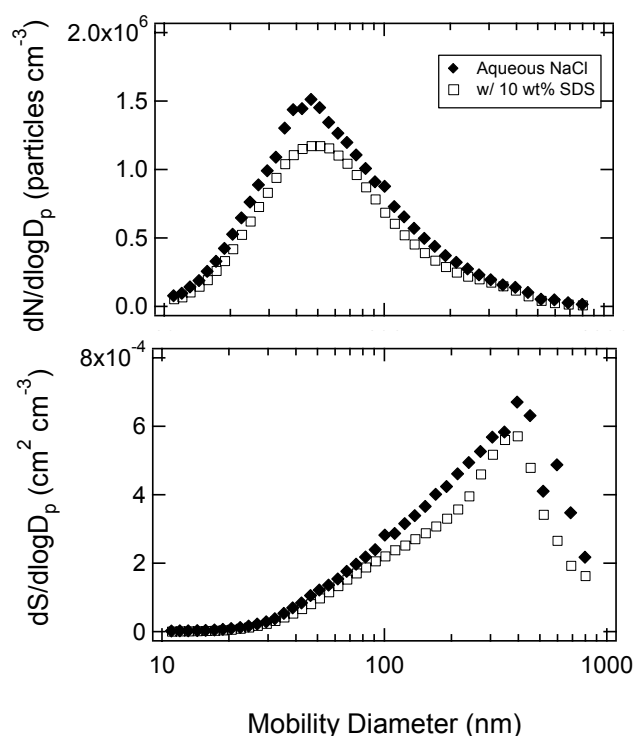


Fig. 1. Representative number (top panel) and surface area-weighted (bottom panel) aerosol size distributions for aqueous NaCl aerosol at 61% *RH* with and without 10 wt% SDS present. Both populations represent $\sim 1.2 \times 10^{-3}$ cm² cm⁻³ total aerosol surface area.

2.3 Flow tube reactor

The kinetics flow tube reactor consisted of a vertically oriented Pyrex tube, 90 cm long, with an internal radius of 1.5 cm. To minimize wall reactions, the inner wall of the flow tube was coated with halocarbon wax and rinsed with water and methanol between sets of experiments. The *RH*-equilibrated aerosol stream was introduced at the top of the flow tube through a perpendicular side-arm. N₂O₅ was introduced via an injector consisting of a 3 mm OD PFA tube housed inside a moveable 6 mm stainless steel tube for structural support. The injector position was changed to vary reaction time and thus obtain kinetic information. All experiments were performed at ambient temperature (295 K) and pressure (760 Torr). The flow velocity down the tube was maintained by a critical orifice located at the bottom of the flow tube, in front of the low pressure CIMS region, which drew 1.6 slpm. An additional 0.3 slpm was drawn by the DMA/CPC. Thus the total flow in the flow tube was 1.9 slpm, resulting in a flow velocity of 4.5 cm s⁻¹. In order to study kinetics under well-mixed, fully developed laminar flow conditions, experiments were limited to the region between 30–75 cm.

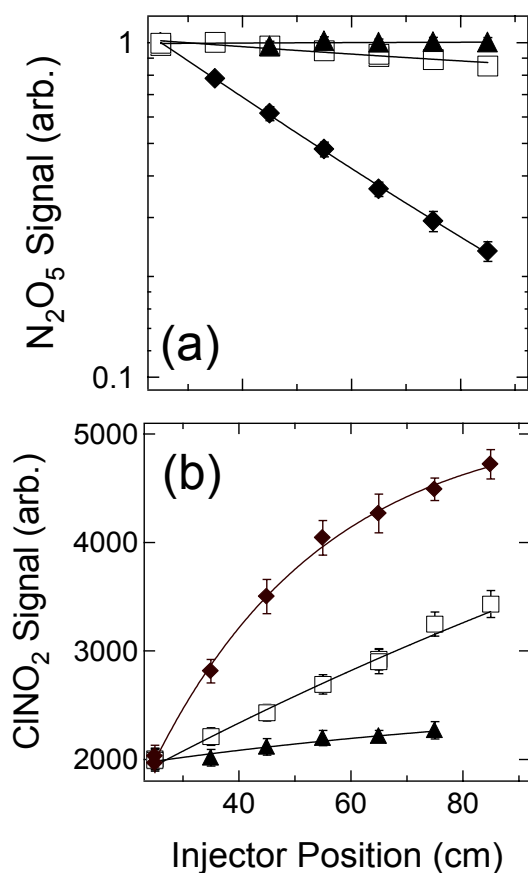


Fig. 2. Representative (a) N_2O_5 decays and (b) ClNO_2 growth curves for ~ 22 ppb N_2O_5 initially present and 62% RH . Signal is plotted versus the injector position in the flow tube. Shown are wall loss (\blacktriangle), reaction with NaCl aerosol (\blacklozenge), and reaction with NaCl aerosol containing 10 wt% SDS (\square). Total aerosol surface area was $S_a = 1.3 \times 10^{-3} \text{ cm}^2 \text{ cm}^{-3}$ for both aerosol decays, and the wall loss was obtained immediately prior to the SDS-doped aerosol run.

2.4 CIMS detection of reactants and products

N_2O_5 and ClNO_2 were detected via CIMS using I^- as a reagent ion. I^- was generated by flowing trace amounts of CH_3I in 0.8 slpm N_2 through a ^{210}Po ionizer (NRD) into the chemical ionization region which consists of a 3.8 cm OD stainless steel tube manifold. The ionizer was positioned axially inside this manifold, with the outlet ~ 2.5 cm away from the mass spectrometer front aperture. Flow from the kinetics reactor (1.6 slpm) was introduced upstream of the ionizer outlet. The pressure in the CIMS region was ~ 60 Torr, yielding a reaction time for ion-neutral reactions of ~ 20 ms.

N_2O_5 was monitored as NO_3^- (62 amu), with a sensitivity at 50% RH of 1.6 cps ppt^{-1} . A higher sensitivity can be achieved, but in order to reduce background signal at 62 amu attributed to HNO_3 (Thornton et al., 2003), ion-neutral reaction time was shortened and the electric field inside the collisional dissociation chamber (CDC) was altered from that

which provided optimal N_2O_5 sensitivity. ClNO_2 was monitored as ICl^- (161.9 amu and 163.9 amu), as in Thornton and Abbatt (2005), and also $\text{I}^- \cdot \text{ClNO}_2$ (207.9 and 209.9 amu), the association reaction product with I^- . The ICl^- signal was a constant fraction of the $\text{I}^- \cdot \text{ClNO}_2$ signal (207.9 amu: 161.9 amu = 1.9:1), although this ratio can be expected to depend on the electric field in the CDC. In a control experiment, we found that HCl vapor reacts with I^- to form $\text{I}^- \cdot \text{HCl}$ under our operating conditions. These two observations suggest that the ICl^- signal is uniquely attributable to ClNO_2 (Thornton and Abbatt, 2005).

3 Results

Shown in Fig. 2a is a set of N_2O_5 decays obtained during experiments at 62% RH for which 22 ppb N_2O_5 was initially present. Data are shown for N_2O_5 loss in the absence of aerosol, or “wall loss” (triangles), reaction with NaCl aerosol (diamonds), and reaction with NaCl aerosol containing 10 wt% SDS (open squares). For both aerosol decays, aerosol surface area was $1.3 \times 10^{-3} \text{ cm}^2 \text{ cm}^{-3}$. Signal is plotted on a log scale versus the injector position in the flow tube (distance from the flow tube outlet/CIMS detection inlet). The linearity of the curves suggests first order kinetics. Therefore, first order rate coefficients for N_2O_5 loss, k^I , can be determined from the slopes of the decay curves. The error bars represent the standard deviation in the raw data used in the average, and the signal was corrected for background. In the case of the wall loss decay and the decay on SDS-containing aerosol shown in Fig. 2a, deviation was small enough that the error bars are roughly the size of the data markers. The slope of an error weighted, linear least square fit of each aerosol decay is input into the Brown algorithm (Brown, 1978) in order to correct for non-plug flow conditions with non-zero loss at the reactor wall. Wall loss was small ($k_w < 0.01 \text{ s}^{-1}$) for experiments with NaCl aerosol, and for many decays, negligible. For some decays measured with aerosol containing 3.5–10 wt% SDS, the decay constant was not distinguishable from that of preceding and subsequent wall loss measurements, even if the wall loss was very small. We thus report some $k^I < 0$; although not real, it is indicative of our ability to determine an aerosol-induced loss under these conditions.

Figure 2b shows ClNO_2 evolution versus injector position during the same experiments featured in Fig. 2a. The curves are from weighted non-linear least squares fits to the data using Eq. (1):

$$S^{\text{ClNO}_2} = S_{\infty}^{\text{ClNO}_2} [1 - \exp(-k_p t)] \quad (1)$$

where $S_{\infty}^{\text{ClNO}_2}$ and k_p are adjustable parameters. For first order loss to multiple products, we can expect $k_p = k^I$ (Steinfeld et al., 1999). The first order rate constants obtained from ClNO_2 growth curves and Eq. (2) are in close agreement with those obtained from N_2O_5 decays, exhibiting similar trends

in surface area, with slightly more scatter. On average, k_p were within 20% of the k^I determined simultaneously.

The corrected first order rate constant, k^I , is related to the reaction probability, $\gamma_{\text{obs}}^{\text{N}_2\text{O}_5}$, according to

$$k^I = \frac{\gamma_{\text{obs}}^{\text{N}_2\text{O}_5} \omega S_a}{4} \quad (2)$$

where ω is the molecular velocity of N_2O_5 and S_a is the aerosol surface area per volume. Equation (2) is only an approximation, but effects due to gas-phase diffusion limitations and modification of the collision frequency due to a net reactive flux to the aerosol are negligible for the small aerosol and moderate reactive uptake coefficients determined here. Shown in Fig. 3 are the corrected first order rate constants for reaction of N_2O_5 with aqueous NaCl aerosol (diamonds) and aqueous NaCl aerosol containing 10 wt% SDS (open squares) as a function of aerosol surface area. Data obtained at various relative humidities are shown together on the same plot, since no relative humidity dependence was observed for RH above 50%, with or without SDS present (see Table 1). Error bars shown represent the 1σ standard deviation in the raw data propagated through the weighted linear least squares fit and the Brown correction. The lines shown were obtained from weighted linear least squares fits to the data. The 1σ confidence limits for the fits are also shown as grey lines. For reaction with pure aqueous NaCl aerosol, the slope of the weighted linear least squares fit corresponds to a reaction probability of 0.015 ± 0.002 , and for aqueous NaCl aerosol containing 10 wt% SDS, the slope yields $\gamma^{\text{N}_2\text{O}_5} = 0.002 \pm 0.001$. A similar analysis for NSW aerosol yields a $\gamma^{\text{N}_2\text{O}_5}$ of 0.034 ± 0.002 at 60% RH in the absence of SDS, roughly twice that for aqueous NaCl aerosol. Table 1 summarizes $\gamma^{\text{N}_2\text{O}_5}$ determined from individual decays and Eq. (2) for the reaction of N_2O_5 with aqueous NaCl aerosol, NSW aerosol, and these aerosols containing 10 wt% SDS, measured at $\sim 51\%$, $\sim 60\%$, and 71% RH .

Figure 4a shows $\gamma^{\text{N}_2\text{O}_5}$ determined at $\sim 60\%$ RH for both aqueous NaCl (diamonds) and NSW aerosol (circles) versus SDS concentration, which ranges from 0.1 to 10 wt% (0.00176 M–0.176 M SDS) depending on the SDS concentration used in the atomizer solution. For comparison, NaCl is estimated to be 8.8 M (Tang et al., 1997) under these conditions. For aqueous NaCl aerosol, when 0.1 wt% SDS is present in the aerosol, no effect is observed, i.e. $\gamma^{\text{N}_2\text{O}_5}$ is the same as when no SDS is present. Starting at 0.3 wt% SDS in the aerosol, $\gamma^{\text{N}_2\text{O}_5}$ is reduced by a factor of 3 relative to no SDS present, and decreases further with increasing SDS concentration until ~ 3.5 wt% SDS, where $\gamma^{\text{N}_2\text{O}_5} \sim 0.002 \pm 0.001$. Above 3.5 wt% SDS, no further decrease in $\gamma^{\text{N}_2\text{O}_5}$ is observed. A similar suppression in $\gamma^{\text{N}_2\text{O}_5}$ by SDS is observed for aqueous NSW aerosol: at 5.5 wt% SDS, $\gamma^{\text{N}_2\text{O}_5}$ is reduced by a factor of 3 relative to no SDS present, and ultimately $\gamma^{\text{N}_2\text{O}_5} \sim 0.001 \pm 0.001$ at 10 wt% SDS. Figure 4b shows $\gamma^{\text{N}_2\text{O}_5}$ plotted versus estimated overall fractional surface coverage, Θ , which takes into account the distribution

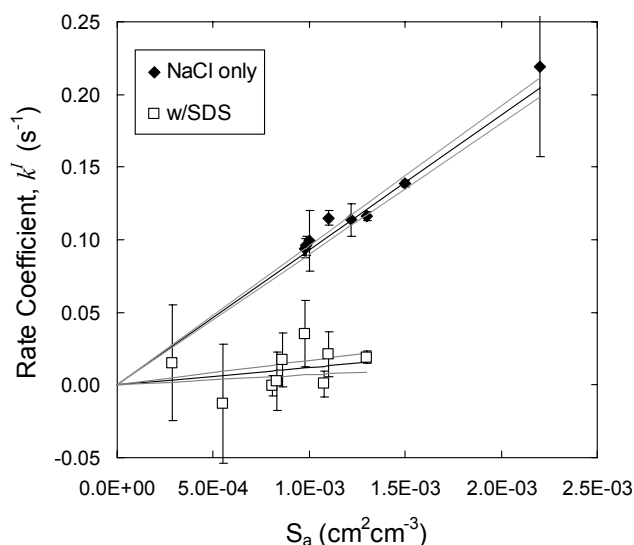


Fig. 3. Corrected first order rate constants for reaction of N_2O_5 with NaCl aerosol (\diamond) and reaction with NaCl aerosol containing 10 wt% SDS (\square) as a function of measured aerosol surface area. Lines shown represent weighted linear least squares fits to the data, with confidence limits of 1σ . For all experiments shown, ~ 22 ppb N_2O_5 was present initially. Data obtained at 51%, 62%, and 72% RH are shown.

Table 1. Reaction probability, $\gamma^{\text{N}_2\text{O}_5}$, as a function of RH for the reaction of N_2O_5 with NaCl aerosol and natural seawater (NSW) aerosol, and for reaction with NaCl and NSW aerosols containing 10 wt% SDS. For all experiments shown, ~ 22 ppb N_2O_5 was present initially, and aerosols are assumed to be aqueous. Each data point represents the weighted average of reaction probabilities from at least three decay experiments at different values of total aerosol surface area.

Aerosol Type	RH (%)	$\gamma^{\text{N}_2\text{O}_5}$
NaCl	51	0.016 ± 0.001
NaCl	61	0.015 ± 0.001
NaCl	71	0.015 ± 0.001
NaCl/10 wt% SDS	50	0.00002 ± 0.001
NaCl/10 wt% SDS	61	0.002 ± 0.001
NaCl/10 wt% SDS	71	0.0005 ± 0.001
NSW	60	0.034 ± 0.002
NSW/10 wt% SDS	60	0.001 ± 0.001

in surface coverages present in each experiment as a result of the polydisperse nature of our aerosol. We discuss our approach to calculating Θ in Sect. 4.2.

The ClNO_2 product yield, Y_{ClNO_2} , was calculated for each decay from the change in N_2O_5 signal and the change in ClNO_2 signal taking into account the combined contributions of the four signals attributable to ClNO_2 signal at 162 amu,

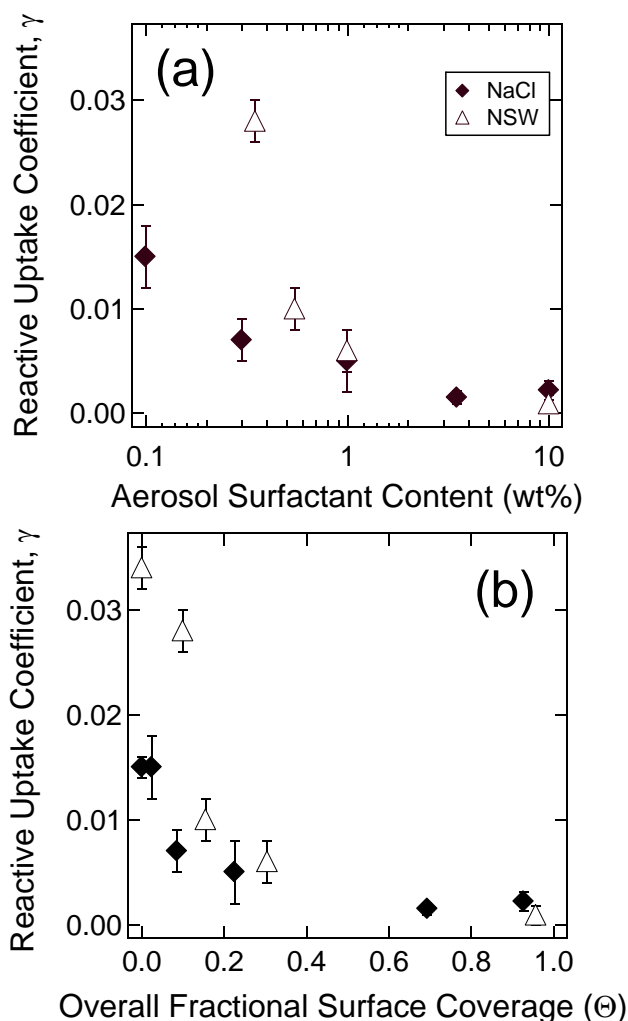


Fig. 4. Reaction probability, $\gamma^{\text{N}_2\text{O}_5}$, is plotted (a) versus SDS concentration in the aerosol and (b) as a function of overall fractional SDS surface coverage in the aerosol population, assuming 1 monolayer = 2×10^{14} molecules cm^{-2} (see text for details). Data shown is for reaction of ~ 22 ppb N_2O_5 with NaCl and natural seawater (NSW) aerosols at 60% RH.

164 amu, 208 amu, and 210 amu as shown in Eq. (3):

$$Y_{\text{ClNO}_2} = \frac{\sum_i \Delta S_{\text{ClNO}_2, i}}{-\Delta S_{\text{N}_2\text{O}_5}} \quad (3)$$

Inherent in this formulation is the assumption that the ClNO_2 ion-molecule reactions proceed at the collision limit, i.e. that detection sensitivity is the same for N_2O_5 and ClNO_2 . This assumption leads to a lower limit estimate of the yield. The ClNO_2 yield was found to be $87 \pm 7\%$ for N_2O_5 reaction on NaCl aerosol, and effectively did not change with the addition of 10 wt% SDS (yield = $85 \pm 6\%$), or with RH. ClNO_2 yield for N_2O_5 reaction on NSW was approximately 80%.

That ClNO_2 was observed at all in the presence of monolayer coverages of SDS suggests N_2O_5 does penetrate to the particle bulk and $\gamma^{\text{N}_2\text{O}_5} > 0$ on the timescales of our experiments.

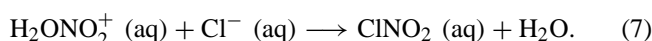
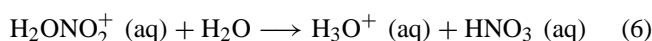
4 Discussion and atmospheric implications

4.1 Kinetics and product yields on pure aqueous NaCl and NSW aerosols

Our measured reactive uptake coefficients for N_2O_5 on aqueous NaCl aerosol fall in between those reported in other studies, which range from ~ 0.004 – 0.03 (Behnke et al., 1997; Schweitzer et al., 1998; Stewart et al., 2004). Behnke et al. (1997) and Stewart et al. (2004) also reported $\gamma^{\text{N}_2\text{O}_5}$ to be independent of RH above 50% RH on aqueous NaCl aerosol. Thornton and Abbatt (2005) measured $\gamma^{\text{N}_2\text{O}_5} = 0.03 \pm 0.008$ on artificial seawater, in close agreement with our measured value of $\gamma^{\text{N}_2\text{O}_5} = 0.034 \pm 0.002$ for aqueous NSW aerosol at 60% RH. Our finding that N_2O_5 is more reactive on aqueous NSW aerosol than on aqueous NaCl aerosol is similar to the findings of Stewart et al. (2004), although the absolute values of our measured $\gamma^{\text{N}_2\text{O}_5}$ are not in good agreement with theirs. It is somewhat surprising that the reaction probability is larger by nearly a factor of 2 on NSW aerosol than on NaCl aerosol, especially when both systems are aqueous. The liquid water content will be very similar for the two aqueous systems, and thus suggests the additional solutes present in seawater (Mg^{2+} , Br^- , etc.) enhance the reactive uptake rate.

It is not surprising that we did not observe signs of suppression of N_2O_5 uptake due to naturally occurring surfactants on the surface of the NSW aerosol used in this study. The seawater was taken from an area with low biological activity and diluted $\sim 10\times$ before atomization. Furthermore, given that the atomizer draws from the bulk of the solution, and that surface active species in seawater are most likely water insoluble (e.g. stearic or palmitic acid), any such surfactants would not be present in the aerosol generated by atomization. We can't rule out the possibility that we might observe suppression if the aerosol were generated via a bubble-breaking mechanism from undiluted seawater sampled during a period of high biological activity (Gershey, 1983; Mochida et al., 2002).

The following mechanism has been proposed for the reaction of N_2O_5 with aqueous NaCl and sea salt aerosols (Thornton et al., 2003; Thornton and Abbatt, 2005):



Our observed ClNO_2 yield of $\sim 90\%$ for N_2O_5 reaction on aqueous NaCl aerosol is consistent with yields of unity reported by Schweitzer et al. (1998), Hoffman et al. (2003), and Behnke et al. (1997) (for their wetted wall flow tube experiments). Behnke et al. (1997) also reported a yield of 65% for their smog chamber measurements using aqueous NaCl aerosol, and attributed the lower value to ClNO_2 loss on the Teflon walls of the chamber. Thornton and Abbatt (2005) reported a yield of $50\pm 10\%$ on artificial seawater aerosol at a single RH, based only on observations of ICl^- . We use a very similar approach and detection technique as was used in that study, except that we were able to measure $\text{I}^- \cdot \text{ClNO}_2$ as well. Given that our present yield determinations of 80% are lower limits, it is likely the true yield on sea salt aerosol is greater than 80% (but less than 100%). N_2O_5 reaction on sea salt aerosol may also produce BrNO_2 (Schweitzer et al., 1998). However, ClNO_2 was the only halogen product detected in this study when using NSW aerosol. According to the above mechanism, a ClNO_2 yield of near unity implies that $K_5k_7[\text{Cl}^-] \gg K_5k_6[\text{H}_2\text{O}]$ (Steinfeld et al., 1999). Thornton et al. (2003) determined a second order hydrolysis rate constant of $2.6 \times 10^4 \text{ M}^{-1} \text{ s}^{-1}$, equivalent to the product K_5k_6 in this mechanism. Using the aerosol concentrations of H_2O and Cl^- at 70% RH, and assuming a value of 2 M atm^{-1} for the Henry's law constant of N_2O_5 (Fried et al., 1994; Jacob, 2000), we estimate that $K_5k_7 \gg 1.8 \times 10^5 \text{ M}^{-1} \text{ s}^{-1}$, or $k_7/k_6 > 10$. K_5 is not known. Such estimates of aqueous phase rate constants are highly uncertain as they carry assumptions about solubility and that mass accommodation is not rate-limiting.

4.2 Effect of aerosol surfactant levels

The presence of SDS leads to a suppression of $\gamma^{\text{N}_2\text{O}_5}$ for both NaCl and NSW aerosol. We observe the onset of suppression, in terms of SDS concentration, to differ between NaCl and NSW aerosol. While some of this difference can be explained by uncertainty in the atomizer SDS concentration, it is possible that the onset of suppression depends partly on the bulk composition of the aerosol. In both systems, $\gamma^{\text{N}_2\text{O}_5}$ decreases with increasing SDS mass fraction until about 3.5 wt% SDS, beyond which no further decrease is observed. This behaviour is suggestive of a monolayer of SDS forming at the gas-aerosol interface, beyond which no further suppression is possible. We examine this aspect in more detail below, but note here that the low values of $\gamma^{\text{N}_2\text{O}_5}$ observed at 3.5–10 wt% SDS are near the limit of detection due to wall loss and the precision in individual decays, so it is possible that $\gamma^{\text{N}_2\text{O}_5}$ could continue to decrease for SDS > 3.5 wt%. The mechanism of suppression could be that SDS inhibits either N_2O_5 uptake from the gas to the bulk aqueous phase, or reactivity by disrupting the distribution of reactants in the bulk or near-surface regions. The fact that the ClNO_2 yield is the same with or without SDS present indicates that both N_2O_5 hydrolysis (Reactions 5 and 6) and the reaction

with Cl^- (Reactions 5 and 7) are inhibited equally. Thus, we conclude that the main effect of the surface organic film is to inhibit the uptake of N_2O_5 from the gas phase by the aqueous bulk.

Surfactants in aqueous solution will partition to the surface until the surface is saturated (Myers, 1988), and in any model system, surfactant concentration at the surface must be treated separately from the bulk monomer concentration (Myers, 1988; Sorjamaa et al., 2004). For ionic single chain surfactants, like SDS or fatty acids, the head group determines how closely the surfactant molecules can pack at the surface (Myers, 1988). The sulfate head group of SDS is most similar to a carboxylic acid, although surfactants typically present in atmospheric aerosol can also have alcohol, aldehyde, ketone, ester, or amine head groups (Gill et al., 1983; Mochida et al., 2002; Peterson and Tyler, 2003; Teruahattu et al., 2002; Russell et al., 2002). Based on studies of dilute SDS-NaCl- H_2O mixtures (Matijevic and Pethica, 1958; Persson et al., 2003), we can assume an SDS footprint of $\sim 50 \text{ \AA}^2$, corresponding to a saturation surface coverage of $2 \times 10^{14} \text{ molecules cm}^{-2}$. At 3.5 wt% SDS, the concentration beyond which we did not observe additional suppression, we predict a surface coverage of $\sim 2 \times 10^{14} \text{ molecules cm}^{-2}$, assuming all SDS partitions to the aerosol surface, and a typical particle surface area of $2.5 \times 10^{-9} \text{ cm}^2$. At the highest SDS concentrations used in this study (10 wt%) we predict a surface coverage of $\sim 5 \times 10^{14} \text{ molecules cm}^{-2}$ if all the SDS partitioned to the surface. This coverage would require an SDS footprint of $\sim 20 \text{ \AA}^2$, which is the tight-packing "Pockels limit" (Pockels, 1891). Whether such a tightly packed film persists in our aerosol or whether SDS loading of the aqueous bulk and possibly micelle formation has begun above 3.5 wt%, we cannot say, but this issue is only relevant for the highest SDS concentration used in this study.

Micelles will form in the solution at bulk surfactant monomer concentrations above what is known as the critical micelle concentration (cmc). Following trends in the cmc of SDS as determined for dilute aqueous NaCl solutions, we expect the cmc to be much less than 10^{-3} M SDS in our 9 M NaCl aerosol (Li et al., 1998; Matijevic and Pethica, 1958). But because of the small size and thus high surface area to volume ratio of our droplets, most SDS molecules present in the aerosol are partitioned to the surface, resulting in bulk monomer concentrations well below the cmc for all runs except that using 10 wt% SDS. If micelle formation has begun at this point, it appears to have no effect on the ability of the monolayer film to act as a barrier to N_2O_5 uptake, as the observed $\gamma^{\text{N}_2\text{O}_5}$ remains nearly a factor of 10 lower than in runs without SDS.

It is particularly intriguing that we observe significant suppression in $\gamma^{\text{N}_2\text{O}_5}$ on both NaCl and NSW aerosol with what can only be sub-monolayer surface coverages of SDS. Due to the polydisperse nature of our aerosol sample, we must take into account a distribution of surface area to volume ratios present for a single population, resulting in a distribution of

SDS surface coverages for a given SDS concentration. If we define θ_i to be the fractional surface coverage of the aerosol in the DMA size bin i , we can estimate the fraction of the total available surface area of our polydisperse aerosol population that is occupied by SDS molecules according to:

$$\Theta = \frac{\sum_i \theta_i N_i}{\sum_i N_i} \quad (8)$$

where N_i is the number density in bin i . Figure 4b shows the data from Fig. 4a plotted as a function of overall fractional surface coverage, Θ , calculated for each point according to Eq. (8), and assuming that all surfactant in the aerosol partitions to the surface until a saturation surface coverage is reached. As noted above, based on the behaviour of $\gamma^{\text{N}_2\text{O}_5}$ we estimate that monolayer coverage corresponds to 2×10^{14} molecules cm^{-2} (3.5 wt% SDS on a 150 nm radius particle). For a given SDS concentration, the standard deviation of Θ due to variation in the particle size distributions between decays was found to be less than 5% of the Θ value. We observe roughly a factor of 3 suppression in $\gamma^{\text{N}_2\text{O}_5}$ at $\sim 8\%$ of a monolayer and 15% of a monolayer for NaCl and NSW aerosol, respectively. If adding SDS molecules to the aerosol surface caused a linear decrease in the accessible aerosol surface area, from Eq. (2) we might expect a linear reduction in $\gamma^{\text{N}_2\text{O}_5}$ with increasing SDS surface coverage. We would then predict a factor of 3 reduction in $\gamma^{\text{N}_2\text{O}_5}$ to correspond to $\sim 65\%$ of a monolayer, i.e. a factor of ~ 5 greater coverage than that at which we observe the reduction. In order to produce a linear dependence of $\gamma^{\text{N}_2\text{O}_5}$ on Θ , it is necessary to set the saturation surface coverage to 5×10^{13} molecules cm^{-2} , a factor of 4 lower than the saturation coverages reported in the literature (Matijevic and Pethica, 1958; Persson et al., 2003). While we can't rule out a larger average footprint for SDS in the highly ionic aerosol used, it seems unlikely for the footprint to be $\sim 200 \text{ \AA}^2$.

Another possible explanation for the observed non-linearity in $\gamma^{\text{N}_2\text{O}_5}$ versus Θ is that fatty acids with 12–15 carbon atoms form “compressible” or “expanded” films (Schofield and Rideal, 1926). Expanded films can be thought of as a disordered transition phase between sparse surface coverage, in which the molecules behave like a 2-D gas, and a tightly packed “incompressible” inverted micelle configuration. Fatty acids with 16 or more carbon atoms form only incompressible films (Schofield and Rideal, 1926; Rosano and La Mer, 1956). We expect SDS to behave similarly to lauric acid (C_{12}) and form an expanded film at sub-monolayer surface coverages. Therefore, the degree of packing and thus the SDS “footprint” will change with increasing surface coverage, resulting in a nonlinear relationship between the number of molecules of SDS on the surface and the degree of inhibition of gas-to-aerosol mass transfer. We know of no other studies showing a reduction in gas-aerosol mass transfer reactive uptake to aerosol due to

sub-monolayer coverages of a surface active organic, but our observations in this regard are consistent with measurements of water evaporation which show that lauric acid in the expanded state exhibits a resistance to mass transfer (Rideal, 1925).

Thornton and Abbatt (2005) found $\gamma^{\text{N}_2\text{O}_5}$ to decrease by a factor of 3–4 in the presence of what they estimated to be monolayer coverage of hexanoic acid. At what we interpret to be full coverage of SDS, we observe greater inhibition of N_2O_5 uptake by a factor of 3 or more relative to their results. Shorter-chain fatty acids such as hexanoic acid are expected to form less tightly packed films (Schofield and Rideal, 1926; Lawrence et al., 2005; Lawrence et al., 2005). Water evaporation studies have found that the resistance to evaporation of water through a fatty acid film was proportional to the compressibility of the film (Rosano and La Mer, 1956), and generally, resistance increases with increasing carbon chain length. Although we do not have molecular-level information about the surface films in this experiment or those of Thornton and Abbatt (2005), it seems reasonable to conclude that the same resistance behaviour is true for N_2O_5 transfer to the aerosol surface.

4.3 Atmospheric implications

This work, together with the studies available in the literature, supports the conclusion that the presence of a sufficiently long-chain surfactant coating creates a resistance to the transfer of gas phase species to and from the aerosol surface (Andrews and Larson, 1993; Thornton and Abbatt, 2005; Garland et al., 2005). Our results suggest that even small quantities of C_{12} – C_{15} surfactants on the surface of aqueous atmospheric aerosol have the potential to inhibit surface processing via formation of expanded films. We conclude that, under conditions where an effective surfactant barrier on aqueous aerosol exists, NO_x lifetimes will increase, and in the case of marine aerosol, halogen activation by N_2O_5 will be suppressed. Such films could also affect the rate of other important multiphase processes, such as SO_2 oxidation. The potential for $\gamma^{\text{N}_2\text{O}_5}$ to be highly variable and dependent on the speciation and mixing state of aerosol organic matter poses a challenge for accurate parameterization of this process in models. It appears that $\gamma^{\text{N}_2\text{O}_5}$ is a useful indicator of organic aerosol phase and mixing states, and together with detailed information on aerosol composition, could be used to infer the prevalence of surfactant barriers in atmospheric aerosol.

Water evaporation studies indicate that long-chain fatty acids could be even more efficient barriers to gas-aerosol mass transfer (Rosano and La Mer, 1956) than the shorter-chained proxy surfactants used in this study and Thornton and Abbatt (2005). However, since long-chain fatty acids ($> \text{C}_{16}$) form tightly packed, incompressible films even at low surface concentrations, higher surfactant concentrations may be necessary before an effect is observed. The most

realistic scenario for atmospheric aerosol would be a mixed surfactant film containing both long- ($>C_{16}$) and shorter-chained surfactants. Such films have been shown to have a resistance to water evaporation intermediate between those of the single-component films (Rosano and La Mer, 1956). It is also important to note that any surfactants on aerosol surfaces would be exposed to the oxidants in the atmosphere, leading to oxidation and possible shortening of the carbon chains (Bertram et al., 2001; Molina et al., 2004). Shortening of the carbon chains of long chain fatty acids ($>C_{16}$) could increase the effectiveness of the surface layer as a barrier to uptake from the gas phase by inducing the formation of expanded films. Further shortening of the chain length ($<C_{12}$) would likely lead to volatilization of the surfactant layer, or reduced surface-activity, depending on the functional groups of the product and the details of the oxidation pathway. Complete volatilization of saturated alkyl surfactants would be expected to occur on a time scale of a few days, which is on the order of the expected lifetime of submicron aerosol (Molina et al., 2004). Experiments to assess the effect of film oxidation on reactive uptake are currently underway.

Acknowledgements. This work was funded in large part by a grant from the Office of Earth Science (NIP/03-0000-0025) at the National Aeronautics and Space Administration (NASA).

Edited by: J. N. Crowley

References

- Andrews, E. and Larson, S. M.: Effect of Surfactant Layers on the Size Changes of Aerosol Particles As A Function of Relative-Humidity, *Environ. Sci. Technol.*, 27, 5, 857–865, 1993.
- Archer, R. J. and La Mer, V. K. The rate of evaporation of water through fatty acid monolayers, *J. Phys. Chem.*, 59, 200–208, 1955.
- Behnke, W., George, C., Scheer, V., and Zetzsch, C.: Production and decay of $ClNO_2$ from the reaction of gaseous N_2O_5 with NaCl solution: Bulk and aerosol experiments, *J. Geophys. Res.-Atmos.*, 102(D3), 3795–3804, 1997.
- Bertram, A. K., Ivanov, A. V., Hunter, M., Molina, L. T., and Molina, M. J.: The reaction probability of OH on organic surfaces of tropospheric interest, *J. Phys. Chem. A*, 105, 41, 9415–9421, 2001.
- Blanchard, D. C.: Sea-to-Air Transport of Surface Active Material, *Science*, 146, 3642, 396–397, 1964.
- Brown, R. L.: Tubular Flow Reactors with 1st-Order Kinetics, *J. Res. Natl. Bur. Stand.*, 83(1), 1–8, 1978.
- Cavalli, F., Facchini, M. C., Decesari, S., Mircea, M., Emblico, L., Fuzzi, S., Ceburnis, D., Yoon, Y. J., O'Dowd, C. D., Putaud, J. P., and Dell'Acqua, A.: Advances in characterization of size-resolved organic matter in marine aerosol over the North Atlantic, *J. Geophys. Res.-Atmos.*, 109(D24), D24215, doi:10.1029/2004JD005137, 2004.
- Cziczo, D. J. and Abbatt, J. P. D.: Infrared observations of the response of NaCl, $MgCl_2$, NH_4HSO_4 , and NH_4NO_3 aerosols to changes in relative humidity from 298 to 238 K, *J. Phys. Chem. A*, 104(10), 2038–2047, 2000.
- Duce, R. A., Mohnen, V. A., Zimmerman, P. R., Grosjean, D., Cautreels, W., Chatfield, R., Jaenicke, R., Ogren, J. A., Pellizzari, E. D., and Wallace, G. T.: Organic Material in the Global Troposphere, *Rev. Geophys.*, 21(4), 921–952, 1983.
- Ellison, G. B., Tuck, A. F., and Vaida, V.: Atmospheric processing of organic aerosols, *J. Geophys. Res.-Atmos.*, 104(D9), 11 633–11 641, 1999.
- Folkers, M., Mentel, T. F., and Wahner, A.: Influence of an organic coating on the reactivity of aqueous aerosols probed by the heterogeneous hydrolysis of N_2O_5 , *Geophys. Res. Lett.*, 30(12), 1644–1647, 2003.
- Fried, A., Henry, B. E., Calvert, J. G., and Mozurkewich, M.: The Reaction Probability of N_2O_5 with Sulfuric-Acid Aerosols at Stratospheric Temperatures and Compositions, *J. Geophys. Res.-Atmos.*, 99(D2), 3517–3532, 1994.
- Garland, R. M., Wise, M. E., Beaver, M. R., Dewitt, H. L., Aiken, A. C., Jimenez, J. L., and Tolbert, M. A.: Impact of palmitic acid coating on the water uptake and loss of ammonium sulfate particles, *Atmos. Chem. Phys.*, 5, 1951–1961, 2005.
- Gershay, R. M.: Characterization of Seawater Organic-Matter Carried by Bubble-Generated Aerosols, *Limnol. Ocean.*, 28(2), 309–319, 1983.
- Gill, P. S., Graedel, T. E., and Weschler, C. J.: Organic Films on Atmospheric Aerosol-Particles, Fog Droplets, Cloud Droplets, Raindrops, and Snowflakes, *Rev. Geophys.*, 21(4), 903–920, 1983.
- Hoffman, R. C., Kaleuati, M. A., and Finlayson-Pitts, B. J.: Knudsen cell studies of the reaction of gaseous HNO_3 with NaCl using less than a single layer of particles at 298 K: A modified mechanism, *J. Phys. Chem. A*, 107(39), 7818–7826, 2003.
- Jacob, D. J.: Heterogeneous chemistry and tropospheric ozone, *Atmos. Environ.*, 34(12–14), 2131–2159, 2000.
- Jacobson, M. C., Hansson, H. C., Noone, K. J., and Charlson, R. J.: Organic atmospheric aerosols: Review and state of the science, *Rev. Geophys.*, 38(2), 267–294, 2000.
- Lawrence, J. R., Glass, S. V., and Nathanson, G. M.: Evaporation of water through butanol films at the surface of supercooled sulfuric acid, *J. Phys. Chem. A*, 109(33), 7449–7457, 2005a.
- Lawrence, J. R., Glass, S. V., Park, S. C., and Nathanson, G. M.: Surfactant control of gas uptake: Effect of butanol films on HCl and HBr entry into supercooled sulfuric acid, *J. Phys. Chem. A*, 109(33), 7458–7465, 2005b.
- Li, Z. D., Williams, A. L., and Rood, M. J.: Influence of soluble surfactant properties on the activation of aerosol particles containing inorganic solute, *J. Atmos. Sci.*, 55(10), 1859–1866, 1998.
- Matijevic, E. and Pethica, B. A.: The properties of ionized monolayers, Part 1. Sodium dodecyl sulfate at the air/water interface, *Trans. Faraday Soc.*, 54, 1383–1389, 1958.
- Mayol-Bracero, O. L., Rosario, O., Corrigan, C. E., Morales, R., Torres, I., and Perez, V.: Chemical characterization of submicron organic aerosols in the tropical trade winds of the Caribbean using gas chromatography/mass spectrometry, *Atmos. Environ.*, 35(10), 1735–1745, 2001.
- McMurry, P. H.: A review of atmospheric aerosol measurements, *Atmos. Environ.*, 34(12–14), 1959–1999, 2000.
- Mmerekki, B. T. and Donaldson, D. J.: Direct observation of the kinetics of an atmospherically important reaction at the air-aqueous

- interface, *J. Phys. Chem. A*, 107(50), 11 038–11 042, 2003.
- Mmereki, B. T., Donaldson, D. J., Gilman, J. B., Eliason, T. L., and Vaida, V.: Kinetics and products of the reaction of gas-phase ozone with anthracene adsorbed at the air-aqueous interface, *Atmos. Environ.*, 38(36), 6091–6103, 2004.
- Mochida, M., Kitamori, Y., Kawamura, K., Nojiri, Y., and Suzuki, K.: Fatty acids in the marine atmosphere: Factors governing their concentrations and evaluation of organic films on sea-salt particles, *J. Geophys. Res.-Atmos.*, 107(D17), 4325–4334, 2002.
- Molina, M. J., Ivanov, A. V., Trakhtenberg, S., and Molina, L. T.: Atmospheric evolution of organic aerosol, *Geophys. Res. Lett.*, 31(22), 4325–4334, doi:10.1029/2004GL020910, 2004.
- Myers, D.: *Surfactant science and technology*, VCH, New York, 1988.
- O'Dowd, C. D., Facchini, M. C., Cavalli, F., Ceburnis, D., Mircea, M., Decesari, S., Fuzzi, S., Yoon, Y. J., and Putaud, J. P.: Biogenically driven organic contribution to marine aerosol, *Nature*, 431(7009), 676–680, 2004.
- Persson, C. M., Jonsson, A. P., Bergstrom, M., and Eriksson, J. C.: Testing the Gouy-Chapman theory by means of surface tension measurements for SDS-NaCl-H₂O mixtures, *J. Colloid Interface Sci.*, 267(1), 151–154, 2003.
- Peterson, R. E. and Tyler, B. J.: Surface composition of atmospheric aerosol: individual particle characterization by TOF-SIMS, *Appl. Surf. Sci.*, 203, 751–756, 2003.
- Pockels, A.: Surface tension, *Nature*, 43, 437–439, 1891.
- Rehfeld, S. J.: Adsorption of sodium dodecyl sulfate at various hydrocarbon-water interfaces, *J. Phys. Chem.*, 71, 738–745, 1967.
- Rideal, E. K.: On the influence of surface films in the evaporation of water, *J. Phys. Chem.*, 29, 1585–1588, 1925.
- Rogge, W. F., Mazurek, M. A., Hildemann, L. M., Cass, G. R., and Simoneit, B. R. T.: Quantification of Urban Organic Aerosols at A Molecular-Level – Identification, Abundance and Seasonal-Variation, *Atmos. Env. A*, 27(8), 1309–1330, 1993.
- Rosano, H. L. and La Mer, V. K.: The Rate of Evaporation of Water Through Monolayers of Esters, Acids, and Alcohols, *J. Phys. Chem.*, 60, 348–353, 1956.
- Russell, L. M., Maria, S. F., and Myneni, S. C. B.: Mapping organic coatings on atmospheric particles, *Geophys. Res. Lett.*, 29(16), 1779, doi:10.1029/2002GL014874, 2002.
- Saxena, P. and Hildemann, L. M.: Water-soluble organics in atmospheric particles: A critical review of the literature and application of thermodynamics to identify candidate compounds, *J. Atmos. Chem.*, 24(1), 57–109, 1996.
- Schofield, R. K. and Rideal, E. K.: The Kinetic Theory of Surface Films – Part II. Gaseous, Expanded, and Condensed Films, *Proc. R. Soc.*, 110A, 167–177, 1926.
- Schweitzer, F., Mirabel, P., and George, C.: Multiphase chemistry of N₂O₅, ClNO₂, and BrNO₂, *J. Phys. Chem. A*, 102(22), 3942–3952, 1998.
- Sorjamaa, R., Svenningsson, B., Raatikainen, T., Henning, S., Bilde, M., and Laaksonen, A.: The role of surfactants in Kohler theory reconsidered, *Atmos. Chem. Phys.*, 4, 2107–2117, 2004.
- Steinfeld, J. I., Francisco, J. S., and Hase, W. L.: *Chemical kinetics and dynamics*, Prentice Hall, Upper Saddle River, N.J., 1999.
- Stewart, D. J., Griffiths, P. T., and Cox, R. A.: Reactive uptake coefficients for heterogeneous reaction of N₂O₅ with submicron aerosols of NaCl and natural sea salt, *Atmos. Chem. Phys.*, 4, 1381–1388, 2004.
- Tang, I. N., Tridico, A. C., and Fung, K. H.: Thermodynamic and optical properties of sea salt aerosols, *J. Geophys. Res.-Atmos.*, 102(D19), 23 269–23 275, 1997.
- Tervahattu, H., Hartonen, K., Kerminen, V. M., Kupiainen, K., Aarnio, P., Koskentalo, T., Tuck, A. F., and Vaida, V.: New evidence of an organic layer on marine aerosols, *J. Geophys. Res.-Atmos.*, 107(D16), 4319–4325, 2002.
- Thornton, J. A. and Abbatt, J. P. D.: N₂O₅ Reaction on Sub-micron Sea Salt Aerosol: Effect of Surface Active Organics, *J. Phys. Chem. A*, ASAP article, doi:10.1021/jp054183t, 2005.
- Thornton, J. A., Braban, C. F., and Abbatt, J. P. D.: N₂O₅ hydrolysis on sub-micron organic aerosols: the effect of relative humidity, particle phase, and particle size, *Phys. Chem. Chem. Phys.* 5, 20, 4593–4603, 2003.